Identification of fracture process under moisture variation in wood materials

Frédéric Dubois[1,*], Rostand Moutou Pitti[2,3,4], Eric Fournely[2,3], Destrebecq JF[2,3]

[1] Heterogeneous Material Research Group, Civil Engineering and Durability department, University of Limoges, Egletons, 19300, France
[2] Clermont Université, Université Blaise Pascal, Institut Pascal, BP 10448, F-63000 CLERMONT-FERRAND, France
[3] CNRS, UMR 6602, IP, F-6317, Aubière, France
F-63000, Clermont-Ferrand, France
[4] CENAREST, IRT, BP 14070, Libreville, Gabon
* Corresponding author: frédéric.dubois@unilim.fr

Abstract The instantaneous fracture of wood material is commonly the source of important accident in the mechanical industries and civil engineering structures. This fact proves that it is necessary to propose a model capable to identify or predict the crack initiation in such materials. In this work, an analytical and numerical model taking into account the stress relaxation coupled with hygrothermal effects and an ageing viscoelastic behavior is proposed. This approach includes shrinkage – swelling effects with orthotropy properties in the radial and transversal directions. This model is applied to a green wood slice during the natural drying process. The viscoelastic properties inducing a partial hydric stress relaxation and a finite element model is proposed based on a orthotropic generalized Kelvin Voigt model taking into account a moisture content dependence on its rheological properties as mechano-sorptive effects. The fracture criterion is introduced according to the Tsai-Wu or Hill approaches rewritten in terms of energy criterion and the numerical model allows to focusing the crack growth initiation localization. Some experimental results are compared with numerical modeling to predict the shrinkage process integrating the crack growth initiation.

Keywords Green wood drying, experimental characterization, finite element method, crack growth initiation

1. Introduction

Aided by its environmental benefits, the wood material is widely used in engineering structures and also, in civil and industrial buildings. As structure element, this material is often machined after drying but also immediately after cutting as green wood. However, the natural or artificial shrinkage due to drying process is commonly responsible of deformations and crack appears in wood pieces or timber structures [1]. Among these deformations, the cup, twist, crook and bow are defects due to the moisture variations, and are even more marked on the wood pieces cut up and stored outdoor during a long time. These behaviors are mainly reinforced by the environmental effects, but also by the orthotropic nature, the heterogeneous aspect, and the anisotropic character of the wood material. In this fact, it is essential, for the lumber, to investigate the different processes that lead to these phenomena in this shape of green wood during the drying.
After the tree felling, the wood log starts a drying phase. Initially, we note the diffusion of the free water molecules to reach the fiber saturation point. In a second step, the bound water migrates from the wood heart until the surface. During this phase, wood is subject to shrinkage swelling effect. The orthotropic properties in the radial tangential plane causes strain blockings inducing hygrothermal stresses. Moreover, in the hygroscopic domain, elastic properties are characterized by a moisture content dependence. The coupling between a tension stress increasing and the elastic property evolutions induce a mechano-sorptive process. Simultaneously, during the tree growth, it is usually observed a mechanical state distribution providing maturation stresses.
The moisture content of freshly felled timber varies enormously, so that in the literature, the deformations and the evolution of drying-induced stresses in wood are studied according numerous methods. Thus, analytical approaches have been developed by Cave [2]. Also, the theoretical expression taking into account the drying time of thin lumber has been developed by Bekhta et al. [3]. Dubois et al. [4] have proposed the analytical approach of elastic response in wood under

moisture content variations. In addition, numerical modeling has been used in order to model the alteration of mechanical properties of wood during drying phase or to study the shape of sawn timber subjected to moisture variation. Simultaneously, several authors have coupling numerical and experimental techniques to analyze the shrinkage . Among them, Kowalski et al. [6] have shown the efficiency of the analytical approach for the identification of fracture process in dried wood based on acoustic emission technique; Kowalski et al. have also presented a model of drying providing the evaluation of moisture content distribution in wood during the drying rate periods, with the moisture content at the body surface reaches the fiber saturation point (FSP). In this work, the radial and tangential strains (inducing crack process) due to the natural drying of a green wood slice are investigated by analytical, experimental and numerical methods.
The first part of the paper recalls the experimental setup composed of a green wood slice in Douglas, a high-sensitivity balance and a video camera. The device is based on the mark tracking method composed of an acquisition system date recording the displacement of targets posted on the wood slice during the drying phase. Simultaneously, the sample is placed on an electronically balance providing the weight measure versus time. The second part details the analysis of experimental results; in this case, the evolution of moisture content versus time is posted in order to obtain the PSF. The radial and transversal strains are computed according to an analytical approach based on a mathematical model coming from cylindrical strain calculations. In the last part, this analytical method is coupling with the swelling-shrinkage tensor taking into account an orthotropic configuration. The finite element calculation is limited, in this paper, at an elastic behavior integrating a mechano-sorptive effect. Also the actual numerical model predicts the cracking due to the transversal shrinkage.

2. Experimental setup

The experimental protocol is based on a green wood slice in Douglas fir with a thickness of 30mm just peeled. Sample is initially conditioned in water in order to assure its saturation. As shown in Figure 1, the preparation of the specimen consists of drawing black marks according to a polar reference centered at the sample heart. In a second step, the sample is placed in the experimental chamber in which the temperature of 22°C and a relative humidity of 33%RH are maintained constant. The sample is placed on a precision balance in order to measure the masse evolution during the drying process. In the same time, black marks allow performing a marking tracking protocol in order to record displacements of these marks using the videometric technology [18]. Versus time, sample mass, displacements and the crack evolution are simultaneously recorded until the mass stability corresponding to the moisture content balance. In order to evaluate the average value of moisture content, samples are placed in a 103°C environment by using an oven.

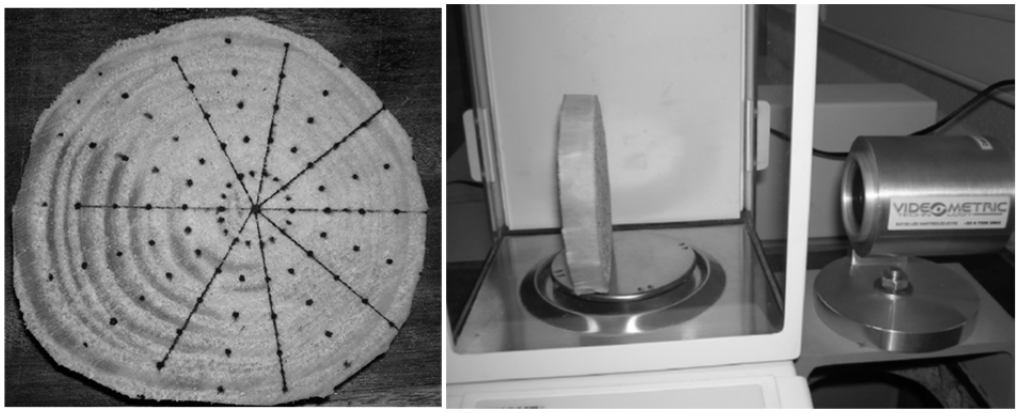

Figure 1. Experimental sample and device

3. Experimental result analysis

3.1. Moisture content evolution

The first results concern the moisture content evolution during drying tests. The graphic in Figure 1 is characterized by a first linear evolution corresponding to the free water migration. At the end of test, we can observe the moisture content equilibrium around 8%. While shrinkage swelling effect start below the fiber point saturation, it is necessary to detect this point. Assuming that the fiber point saturation gives a non linearity in the time moisture content curve, a zoom of the last graph provides an estimation of the specific moisture content value of 30% corresponding to the point saturation fiber limit. This value is further confirmed by studying strain deformations,

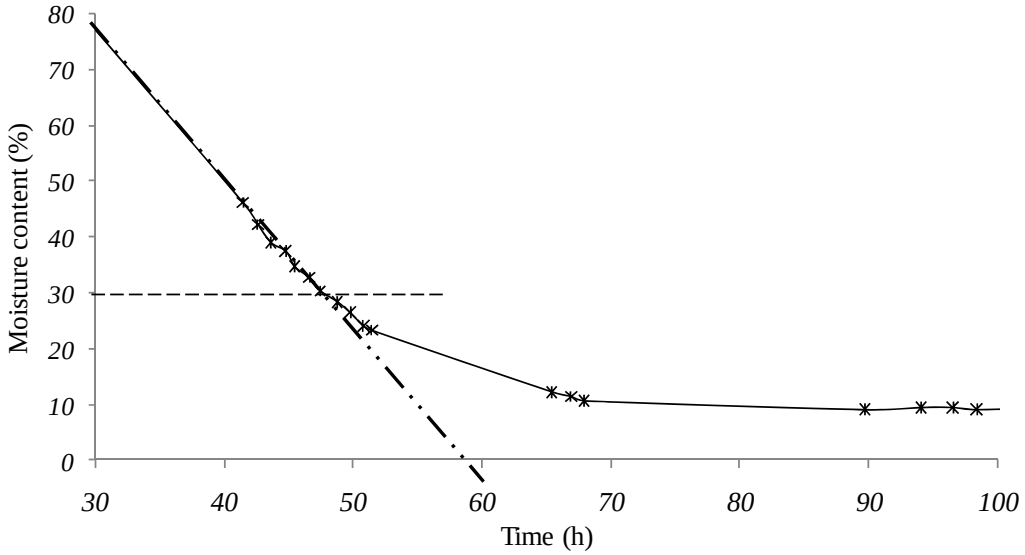

Figure 2. Moisture content evolution and fiber point saturation localization

3.2. Strain evolution

The mark tracking method allows the calculation of displacements of each black mark center. The mechanical exploration requests the definition of strains and, more precisely, radial and tangential components. With this consideration, a specific derivation of displacement fields must be operated. Let us consider a perfect circular slice with a polar referential centered at this center, Figure 3. M' is the image of the displacement of M.

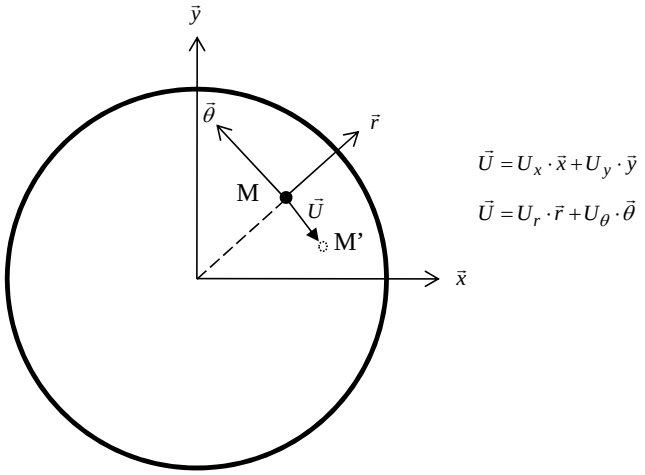

Figure 3. Polar referential in a perfect circular slice

In order to identify each black mark, Figure 4 proposes a notification by the intersection between

radiuses and rings. For example, the mark M_i^j is the point at the intersection between the radius R_i and the ring or crown C_j. Let us note that radial and tangential strains are defined at the middle point comprised between M_1 and M_2. According to this remark, the radial strain is calculated at the point M_2^{1-2} corresponding to a point placed in the radius n°2 and between rings 1 and 2.

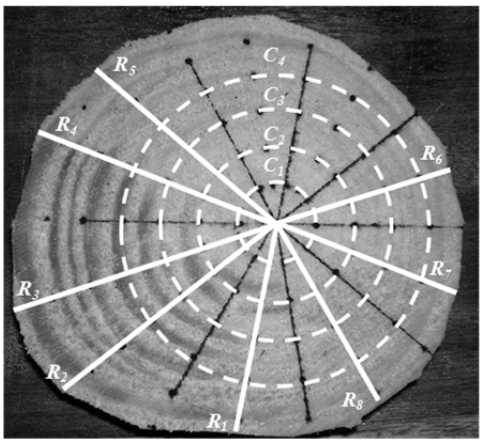

Figure 4. Notification of radius and rings

With the same way, the tangential strain is calculated at the point M_{2-3}^2 placed in the ring n°2 and between radiuses 2 and 3. Figures 5 presents radial strains along radius n°3.

show strain evolution along intermediary radius.

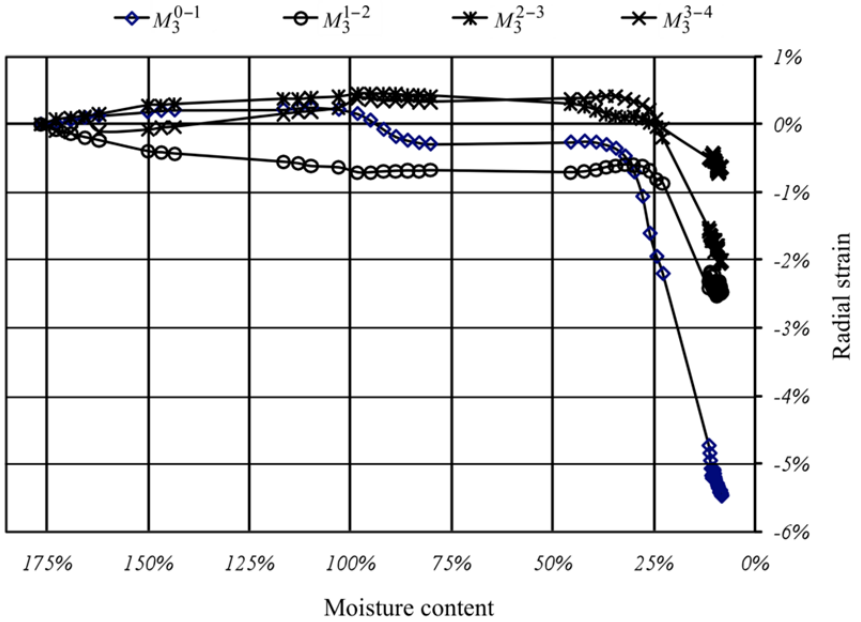

Figure 5. Radial strain along radius n°3

Experimental tangential strains are measured along crowns C_1 to C_5. Firstly, results are presented in terms of tangential strain evolution versus time for points M_{i-j}^l placed in the intersection of crown C_l and the radius comprised between radius R_i and R_j. Figure 6 and 7 show strain evolution along intermediary radius.

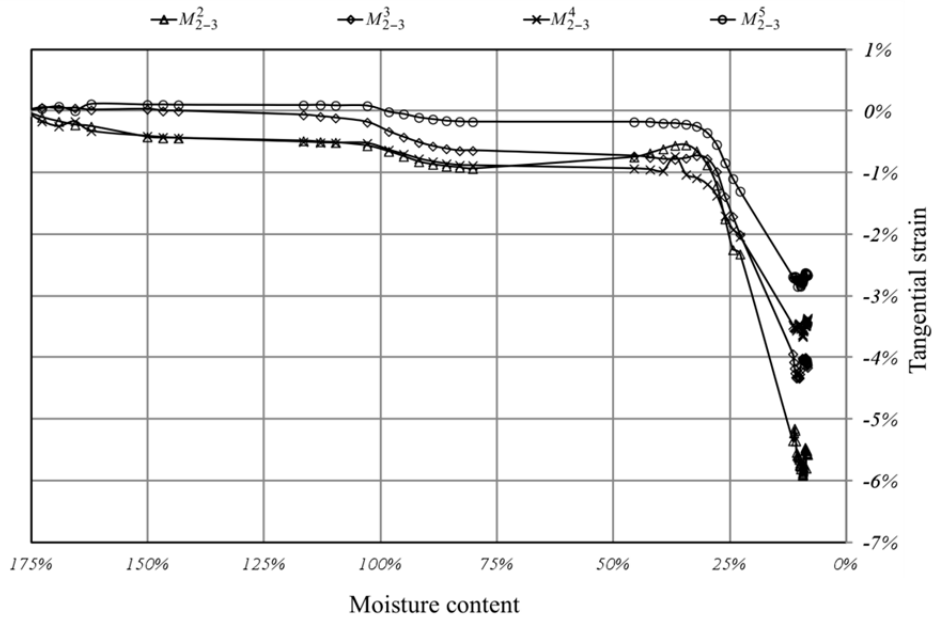

Figure 6. Tangential strains for radius comprised between R_2 and R_3

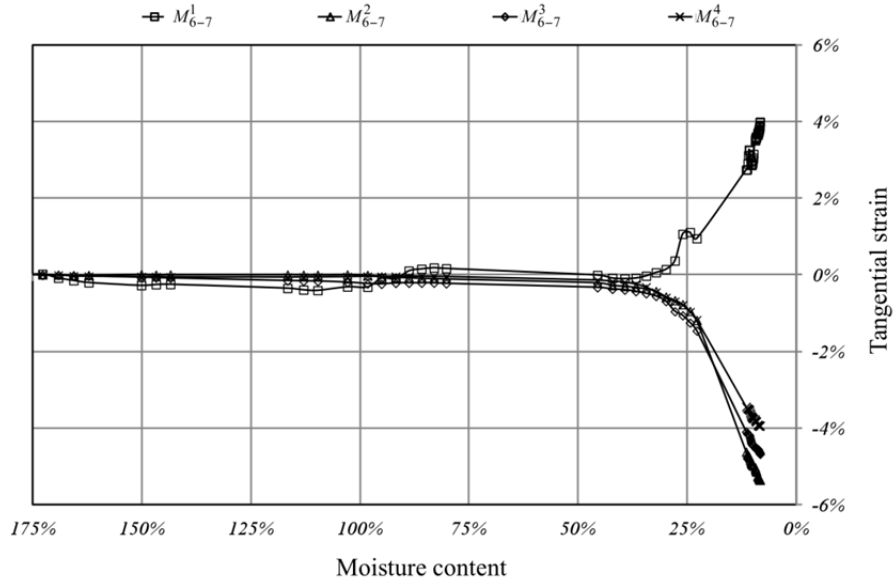

Figure 7. Tangential strains for radius comprised between R_6 and R_7

These results can highlight few points:

- The tangential strains are, in the whole, in a compression increasing during drying process.
- At a moisture content level, the tangential strain seems increasing at the sample center
- An heterogeneity can be observed around the crack initiation vicinity
- Around 18% of moisture content, we can observe a jump of tangential strain valued near the radius R_1 and R_7 near the sample edge which can be explain by the crack growth initiation.

4. Finite element approach

The simulation of the drying process in free disk requests the development of a specific model

taking into account different mechanical behavior such as shrinkage-swelling effects, the elastic property dependence on moisture content and the material orthotropy.

4.1. Mechano-sorptive model

The coupling between moisture content variations and mechanical behavior is based on the addition of shrinkage-swelling response and mechano-sorptive behavior. During drying process, Gril et al. and Husson et al. has putted in evidence one hygro-lock effect affecting elastic and viscoelastic responses [4]. According to a creep representation, the mechanical model can be assimilated by a generalized Kelvin Voigt model in which each springs accept an elastic hygro-lock behavior completed by an uncoupled shrinkage-swelling element as shown in Figure 8 in its uniaxial form.

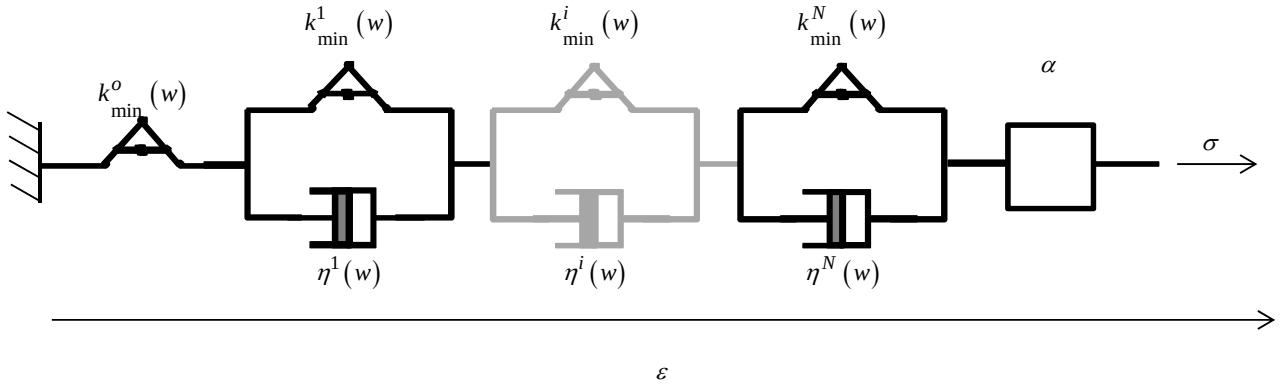

Figure 8. Generalized Kelvin Voigt model with hygro-lock properties

The generalized mechano-sorptive behavior is defined according to the following hereditary integral form:

$$\varepsilon(t)=\int_0^t \frac{1}{k^o_{\min}(\tau,t)}\cdot\frac{\partial\sigma}{\partial\tau}d\tau+\sum_{i=1}^{N}\int_0^t\left[\int_\tau^t \frac{1}{\eta^i(\vartheta)}.\exp^{-\int_\tau^\vartheta \frac{k^i_{\min}(\alpha,t)}{\eta^i(\alpha)}.d\alpha}.d\vartheta\right]\cdot\frac{\partial\sigma}{\partial\tau}.d\tau+\int_0^t\alpha\cdot\frac{\partial w}{\partial\tau}\cdot d\tau \qquad (1)$$

4.2. Incremental formulation

The finite element implementation requests a time incremental formulation allowing the integration, step by step, of the hereditary behavior induced by viscoelastic and hygro-lock effects. The incremental formulation is developed in order to simplify the integral calculus by summarizing complete past history in an additional variable. In this case, the numerical algorithm requests to update mechanical field during a time increment. Let us introduce a time discretization as follow:

$$t_n=t_{n-1}+\Delta t_n \qquad (2)$$

At the time t_n, the strain and mechanical stress can be defined from their value at the time t_{n-1} such as

$$\varepsilon(t_n)=\varepsilon(t_{n-1})+\Delta\varepsilon_n \quad \text{and} \quad \sigma(t_n)=\sigma(t_{n-1})+\Delta\sigma_n \qquad (3)$$

$\Delta\varepsilon_n$ and $\Delta\sigma_n$ are increments of strain and mechanical stress during the time step Δt_n, respectively. The incremental formulation consists on the evaluation of the strain increment according to the following constitutive equation:

$$\Delta\varepsilon_n = A_n \cdot \Delta\sigma_n + \tilde{\varepsilon}\left(t_{n-1}\right) \tag{4}$$

A_n is a pseudo compliance function which enables us to traduce the instantaneous strain response induced by the mechanical stress increment. $\tilde{\varepsilon}_{n-1}$ is the complete past history effects of moisture content and loadings on strains. Finally, the finite element structuring integrates the orthotropic properties in the radial tangential referential. In this condition, the uniaxial incremental formulation (4) can be generalized in the following finite element form:

$$\Delta\underline{\underline{\varepsilon}}_n = \mathbf{A} \cdot \Delta\underline{\underline{\sigma}}_n + \tilde{\underline{\underline{\varepsilon}}}\left(t_{n-1}\right) \tag{5}$$

$\Delta\underline{\underline{\varepsilon}}_n$ and $\Delta\underline{\underline{\sigma}}_n$ designate increments of strain and stress tensors, respectively. In order to solve this equation by a finite element algorithm, let us employ the technique proposed by Ghazlan et al. which is derived from the virtual work principle. If the nodal displacement vector increment is noted $\left\{\Delta U\left(t_n\right)\right\}$, the balance equation, in the discretized domain V, can be written as follow

$$\mathbf{K}_T \cdot \left\{\Delta U\left(t_n\right)\right\} = \left\{\Delta F^{ext}\left(t_n\right)\right\} + \left\{\Delta\tilde{F}\left(t_{n-1}\right)\right\} \tag{6}$$

$\mathbf{K}_T$ is an equivalent tangent matrix assembled from the tensor $\mathbf{A}$.

4.3. Finite element results

As shown in Figure 9, the finite element mesh is realized according to a global positioning system centered on the heart specimen allowing defining the center of the cylindrical orthotropic reference. The contact surface between specimen and balance is operated by blocking its vertical displacements. A referential point is also blocked in its vertically in order to eliminate a rigid body displacement. We assume a perfect slice of this surface according to isostatic boundary conditions. Specific lines (radius and crowns) have been integrated in mesh in order to have a concordance with experimental black mark displacements, Figure 1.

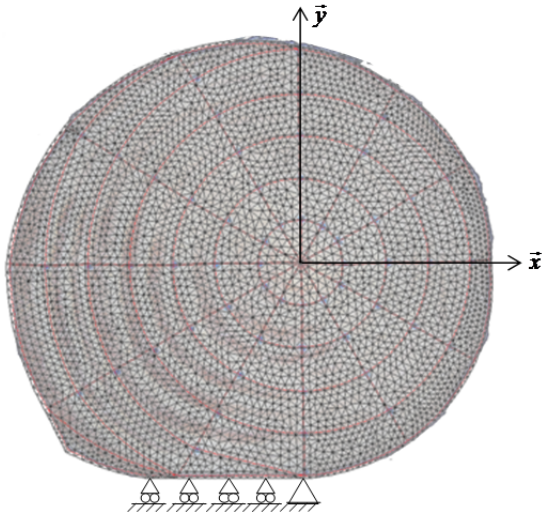

Figure 9. Finite element mesh

According to the last finite element algorithm, mechanical fields are computed versus moisture content level with an increment of 1%. In accordance with Figure 2, the fiber saturation point is assumed to be around 30% inducing representative strain evolutions. All mechanical fields are calculated in the local orthotropic system. For a final moisture content of 8% corresponding to the crack growth initiation, the numerical displacements are plotted in Figure 10 with an amplification factor of 2.

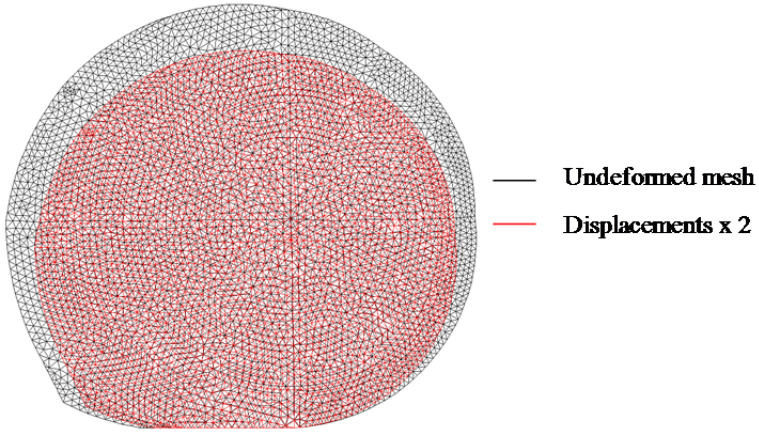

Figure 10. Finite element displacements

Figures 11 and 12 present the comparison between radial and tangential strains given by finite element approach and experimental data. In order to clarify visibility, we choose to represent experimental measurements for extreme rings for radius n°6. For radius n°6, we can observe a very good agreement between experimental and simulation results. However, the results in terms of tangential strains present differences induced by the development of a crack in the end of test. At the moisture content of 8%, mappings of σ_{RR}, σ_{TT} and σ_{RT} are posted in Figures 13 to 15. About radial stresses, we can observe an evolution of heart (compression state) toward outside (tension state) with a radial homogeneity. The combination of tangential and shear stresses illustrates that the crack growth initiation is based on a coupling between tangential tensions and shear state according to a mixed mode configuration.

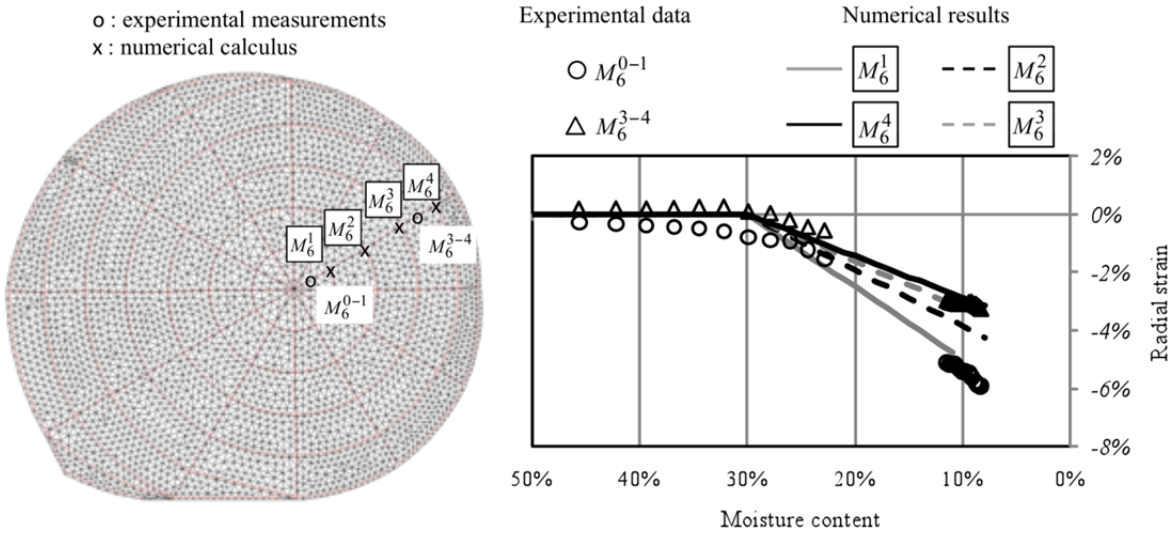

Figure 11. Comparison between experimental and numerical radial strains along radius n°6

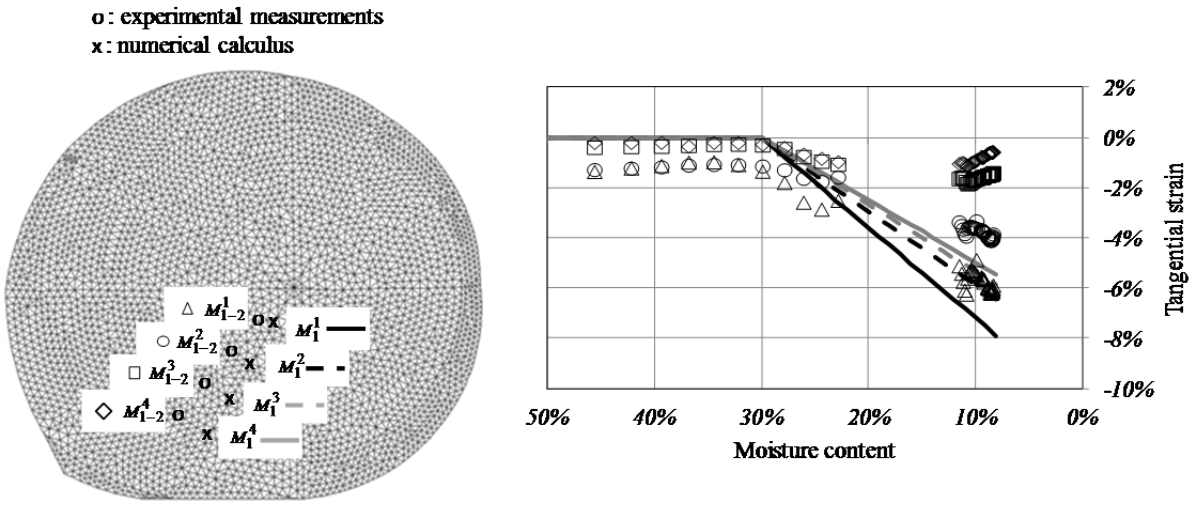

Figure 12. Comparison between experimental and numerical tangential strains along radius n°1

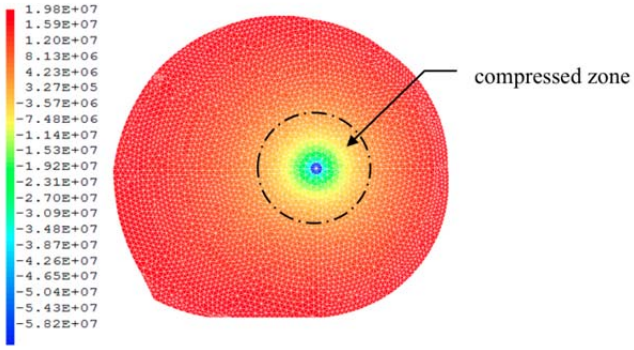

Figure 13. Radial stress mapping at 8% of moisture content

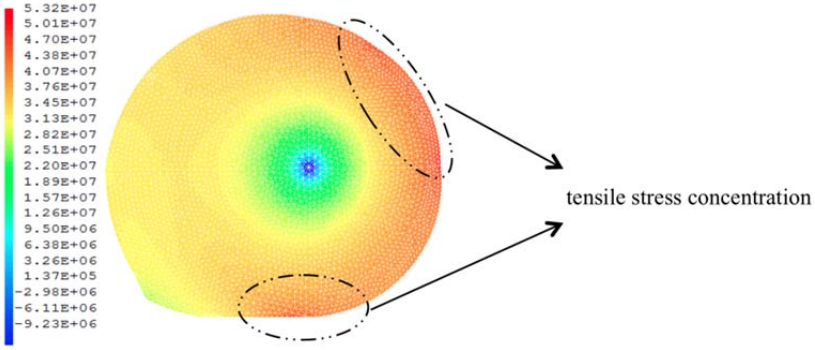

Figure 14. Tangential stress mapping at 8% of moisture content

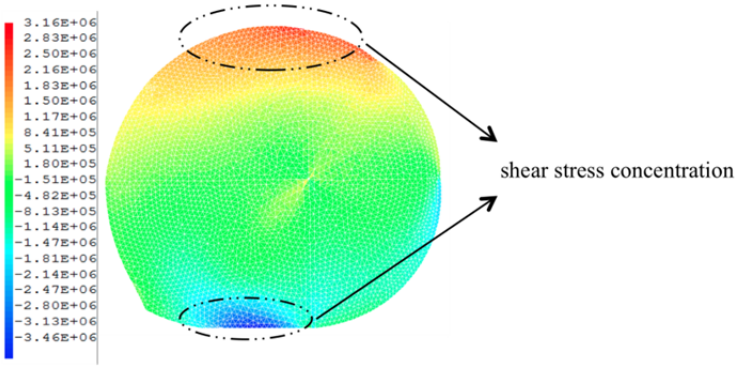

Figure 15. Shear stress mapping at 8% of moisture content

By considering a classical Tsai-Wu's criterion written in a stress form, the Figure 16 shows us the mapping of the function f by noting its concentration in the crack growth zone vicinity.

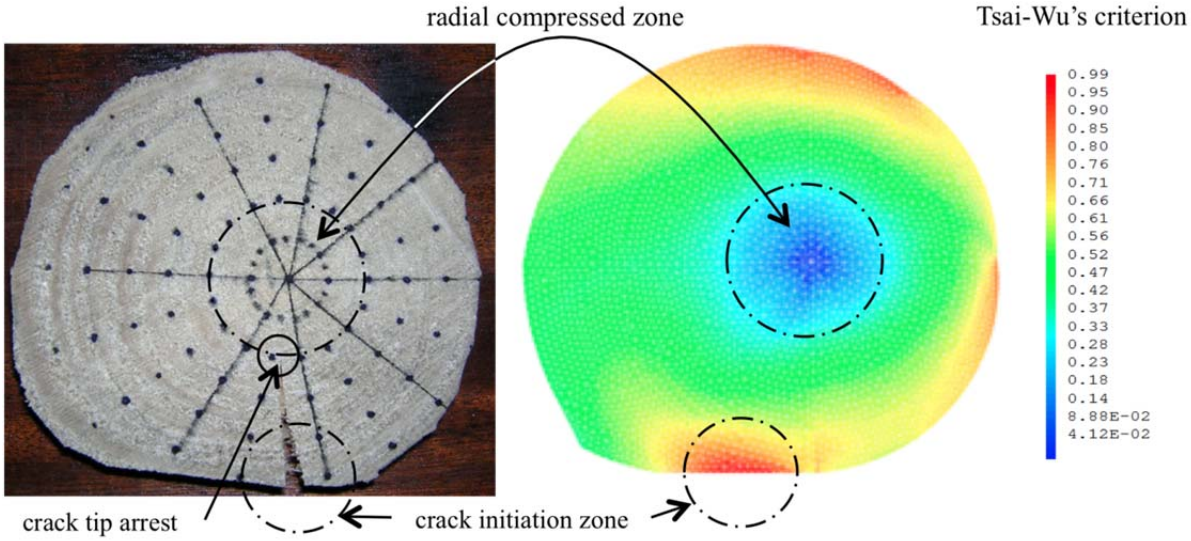

Figure 16. Shear stress mapping at 8% of moisture content

5. Conclusion

The strain and fracture process due to the natural drying of green wood slice have studied in this work. The experimental device, composed of a sensitively balance, a video camera, a slice with tracked, have provided to own the displacement in the slice axis during drying phase. The experimental protocol is completed with a numerical model integrating mechano-sorptive effect. In this context, a finite element model based on an incremental formulation is developed. By using comparisons between finite element results and experimental marker tracking data, the stress field is computed in the cylindrical orthotropic radial-transverse reference by taking into account cylindrical defects induced by conditions of the tree growth. By performing a strength criterion based on Tsai-Wu or Hill approaches, the numerical model allows to focusing the crack growth initiation localization.

References

[1] A.P. Schniewind, R.A. Pozniak, On the fracture toughness of Douglas fir wood, Engineering Fracture Mechanic, 1971, 223–230.
[2] I.D. Cave, A theory of the shrinkage of wood, Wood Science and Technoly, 1972, (6), 284-292.
[3] P. Bekhta, I. Ozarkiv, S. Alavi, S. Hiziroglu, A theoretical expression for drying time of thin lumber, Bioresource Technoly, 2006, (97), 1572–1577.
[4] F. Dubois, J. M. Husson, N. Sauvat, N., Manfoumbi Modeling of the viscoelastic, mechano-sorptive behavior in wood, Mechanics of Time Dependent Materials, doi: 10.1007/s11043-012-9171-3, 2012.
[5] S.J. Kowalski, A. Smoczkiewicz-Wojciechowska, Stresses in dried wood, Modeling and experimentation, Transp Porous Med., 2007, (66), 145-158.